The residual load carrying capacity of timber joints

J.W.G. van de Kuilen
Delft University of Technology, Faculty of Civil Engineering and Geosciences, Delft, The Netherlands
TNO Building and Construction Research, Delft, The Netherlands

Timber joints that have been preloaded for 2 to 8 years have been short term tested in accordance with EN 26891. The applied load levels varied between 30% and 50% of the average short term strength. The study comprised nailed, toothed-plate and split-ring joints. All joints were made of spruce and loaded in tension.
The test results indicated no strength loss during this period. The strength of the preloaded joints was at least equal to the average short term strength of joints with no preloading prior to testing. Actually, the results indicate a slight increase in strength. The development of the strength of the joints in time is modelled with an exponential damage equation. The parameters of the damage equations have been determined on the basis of time to failure tests on the same types of joints.

Key words: **timber joints, residual strength, damage accumulation**

1 Introduction

An important factor in the design procedure of timber structures is the modification factor k_{mod} for duration of load. The factor takes into account that timber has a lower strength if a load is acting over longer periods. According to Eurocode 5 a load has to be assigned to a load duration class depending on the accumulated time period over which the load is acting on the structure.
The design procedure could be enhanced to a more probabilistic based method if accumulated load can be determined as well as the influence on the strength over time. The residual strength, i.e. the remaining strength after being loaded to levels which occur in practice is studied. Information on this matter is useful in the derivation of modification factors and the time boundaries of load duration classes. Another aspect for which this information is useful is the evaluation of existing timber structures. Structures may have been in service for quite some time after which the use of the building is altered and information is needed on the structural safety.
It would be an advantage if the accumulated damage since the erection of the structure can be estimated and if the accumulated damage is negligible that full strength is still available.

2 Test programme

To study the effects of accumulated load on the residual strength tests were started in 1984 to obtain information on the effect of preloading on the strength reduction in time. Test specimens were loaded up to 50% of the average short term strength for several years and the residual strength was then determined in short term tests.
In 1984 nailed, toothed-plate and split-ring joints were loaded to 30, 40 or 50% of the average short term strength. The dimensions and fasteners used, are shown in Annex A.1. The average short term strength values and the respective load values are given in table 1.

Table 1. Load levels for duration of load tests as a percentage of the average short term strength and equivalent loads on the joints.

Load level:	Nailed joints [kN]	Toothed-plate joints [kN]	Split-ring joints [kN]
Average strength	45.0	32.2	28.8
50 %	22.5	16.1	14.4
40 %	18.0	12.9	11.5
30 %	13.5	9.7	8.6

The joints were loaded for a certain period of time, unloaded and then short term tested in a standard short duration (SST) test. Five series were tested and each series comprised the three joint types. Table 2 gives an overview of the five series and the loads and time duration that were applied during the preloading periods.

Table 2. Series with load levels and testing times

Series:	0 - 2 years:	2 - 4 years:	4 - 6 years:	6 - 8 years:
Series 1	50 %	-	-	-
Series 2	40 %	50 %	-	-
Series 3	30 %	40 %	50 %	-
Series 4	30 %	40 %	50 %	50 %
Series 5	50 %	50 %	50 %	50 %

Series 1, 2, and 3 consist of two series of 5 specimens per joint type each. Series 4 and 5 consist of one series of 5 specimens per joint type. The full loading schedules are given in Annex B.1 to B.5. Earlier reports were written by Kuipers and Kurstjens [1984], Kurstjens [1989,1990] and Kurstjens and Stolle [1991].

3 The relation between time to failure and residual load carrying capacity

The time to failure effect in timber relates to the decrease in strength of the material if a load is applied for a certain period of time. To account for this effect, design codes often make use of modification or load-duration factors which take into account the time span of the load. In Eurocode 5 for example a distinction is made between different types of load and from each type of load the accumulated duration is estimated. The longest time span is based on a design reference period of 50 years.

The question is raised what the real strength in the material is during a time to failure test. Does the strength decrease slowly in accordance with the time to failure line, or does it follow a different line? Tests on timber from demolished buildings almost never show a decrease in strength [Kuipers, 1986], [Van Bueren, 1985], [Fridley et al. 1994], indicating that failure occurs in a very short period of the total lifetime and that during most of the lifetime full strength is available. In paragraph 5 an exponential damage model [Gerhards, 1979] is applied to analyse the data.

4 Residual load carrying capacity after creep loading

4.1 Introduction

Over the years, several series of specimens with various loading histories were short term tested to obtain information on the accumulated damage during the creep period. In this chapter the results of these tests are summarized. Preloading periods varied from 2 to 8 years. In Kurstjens, [1989, 1990] and [Kurstjens and Stolle, [1991], the test results of the series that lasted 2 to 6 years have been reported (Series 1, 2 and 3). The test results of the 8 year tests (Series 4 and 5) are reported in paragraph 4.2. The residual strength analysis also includes the earlier test results of joints with different loading histories.

4.2 Residual strength tests of 1994

4.2.1 Nailed joints

Figures 4.1 and 4.2 show the short term test results of the nailed joints that were tested after 8 years at 50% (Series 5) and for 2 years at 30%, 2 years at 40% and 4 years at 50% (Series 4) respectively. The strength values of the individual specimens are given in table 4.1 and 4.2. The average strength F_{avg}, the standard deviation std, and the coefficient of variation cov are also given.

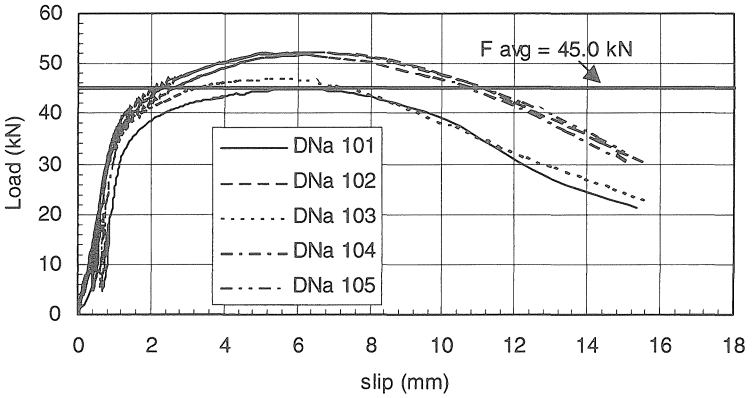

Fig. 4.1 Load displacement curves of nailed joints of series 5.

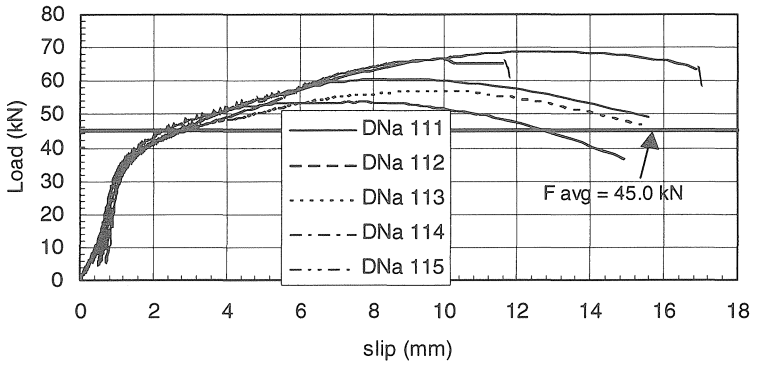

Fig. 4.2 Load displacement curves of nailed joints of series 4.

Table 4.1 Strength values and failure mode of nailed joints of series 5 (μ = 45 kN).

Specimen No.	F_{max} (kN)	Failure mode
DNa 101	44.87	nail bending + splitting
DNa 102	52.32	nail bending + splitting
DNa 103	47.07	nail bending + withdrawal + splitting
DNa 104	51.89	nail bending + withdrawal
DNa 105	52.38	nail bending + withdrawal + splitting
	F_{avg} = 49.71 kN, std = 3.50 kN, cov = 0.07	

Table 4.2 Strength values and failure mode of nailed joints of series 4 (μ = 45 kN).

Specimen No.	F_{max} (kN)	Failure mode
DNa 111	60.74	nail bending + splitting
DNa 112	69.11	nail bending
DNa 113	57.33	nail bending + splitting
DNa 114	53.91	nail bending + withdrawal + splitting
DNa 115	66.85	nail bending + withdrawal + splitting
	F_{avg} = 61.59 kN, std = 6.37 kN, cov = 0.10	

The strength values of series 4 are high compared to the average strength given in table 2.1 and those of series 5. This high strength is attributed to the fact that the nails in these joints were rusted as a result of a broken pipe in the central heating system in the laboratory, resulting in a large amount of warm water overflowing the specimens. The overflow with warm water directly resulted in an increase in displacement measurements of the joints and thus higher creep values. The overflow also resulted in severe rusting of the nails. It is known from practice (p.e. pallets) that rusted nails in general have a higher resistance against withdrawal forces than smooth nails. The average strength value of these 5 joints is 24% higher than the average strength value of the other 5 joints. The test results of series 5 are close to the average short term strength of not-preloaded joints.
Since the failure mode of the nailed joints is a combination of bending of the nails and the consecutive withdrawal from the middle member with splitting of the side members it is not surprising that the specimens DNa 111 to 115 showed significantly higher strength than the specimens DNa 101 to 105.
When splitting occurs, the timber splits in most cases between nails in a side row. Some joints were partly sawn after the short term test and the nail bending pattern was studied. Straight nails, nails with a single plastic hinge and nails with two plastic hinges were observed. In all cases it was uncertain that full plastic hinges had developed. A failure pattern with two plastic hinges resembles the short term failure mode, both experimentally as well as theoretically using the Johansen equations [Johansen, 1949]. Apparently, a creep test of 8 years can be long enough for a specimen to show a transition from one failure mode to another. The creep is responsible for a time dependent change in joint geometry, since the nails will gradually rotate. A short term test is then performed on a specimen with rotated nails, which is different from a specimen where the nails are still in their original position.

4.2.2 Toothed-plate joints

In figure 4.4 and 4.5 the load displacement curves of the toothed-plate joints that were tested for 8 years at 50% (Series 5) and for 2 years at 30%, 2 years at 40% and 4 years at 50% (Series 4) respectively are shown. Failure is initiated by a block shear under the bolt in the middle member. The average drop in strength after the initiation of a shear plug is estimated at about 8.5 kN. The maximum load carrying capacity is generally reached at a slip of less then 5 mm. The strength values of the individual specimens are given in tables 4.5 and 4.6.

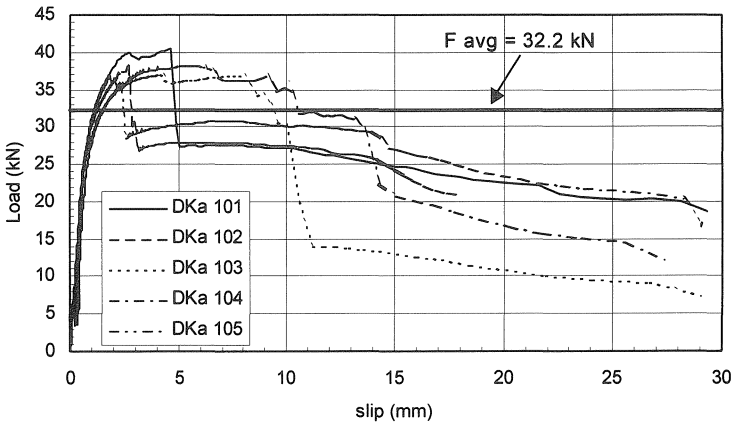

Fig. 4.4 Load displacement curves of toothed plate joints of series 5.

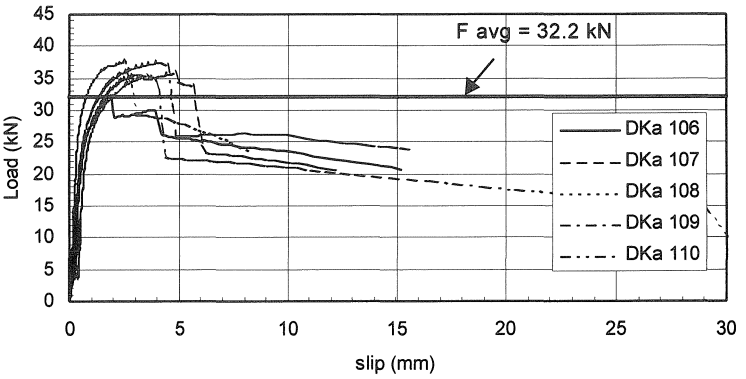

Fig. 4.5 Load displacement curves of toothed-plate joints for series 4.

Table 4.5 Strength values and failure mode of toothed plate joints of series 5 (μ = 32.2 kN).

Specimen No.	F_{max} (kN)	Failure mode
DKa 101	40.54	shear plug of middle member
DKa 102	37.75	shear plug of middle member
DKa 103	36.92	tension failure of middle member
DKa 104	38.24	shear plug of middle member
DKa 105	36.68	shear plug of middle member
	F_{avg} = 38.03 kN, std = 1.54 kN, cov = 0.04	

Table 4.6 Strength values and failure mode of toothed-plate joints of series 4 (μ = 32.2 kN).

Specimen No.	F_{max} (kN)	Failure mode
DKa 106	32.33	shear plug of middle member
DKa 107	35.56	shear plug of middle member
DKa 108	37.51	shear plug of middle member
DKa 109	37.36	shear plug of middle member
DKa 110	35.60	shear plug of middle member
	F_{avg} = 35.67 kN, std = 2.09 kN, cov = 0.06	

All but one specimen failed in shear plug of the middle member. This is the same failure mode as found in a standard short duration test. It is also the same as found in time to failure tests where shear plug under the bolt occurs before the specimen totally fails. It can therefore be concluded that toothed-plate joints do not show a transition in failure mode due to creep loading.

4.2.3 Split-ring joints

In figures 4.6 and 4.7 the load displacement curves of the specimens of series 5 and 4 are shown. After reaching the ultimate load a block shear failure under the bolt occurs.

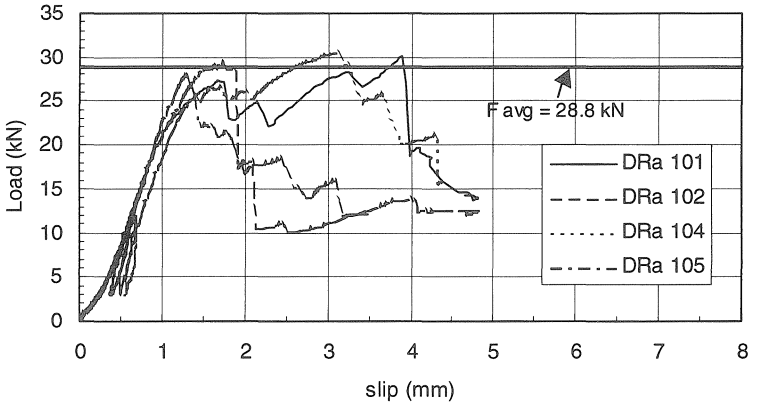

Fig. 4.6 Load displacement curve of split-ring joints of series 5.

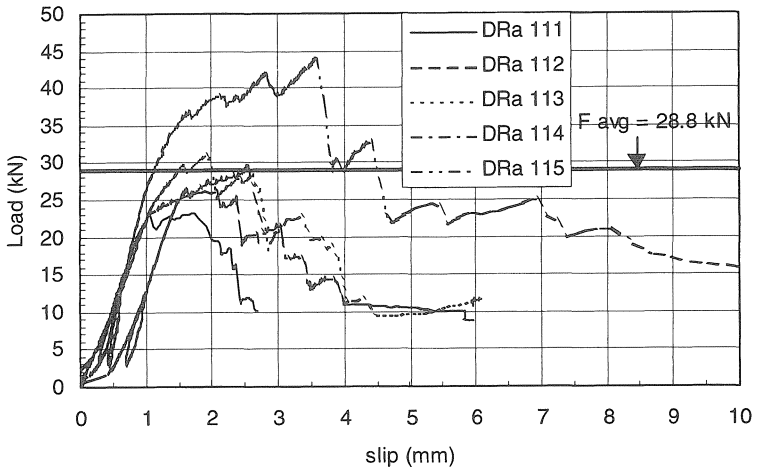

Fig. 4.7 Load displacement curves of split-ring joints of series 4.

The consecutive loads to which the specimens of series 4 was 45%, 40% and 50% instead of the proposed 30%, 40% and 50%. This loading sequence of 45-40-50 is close to an 8 year level of 50%.

The strength values and failure modes of the individual specimens are given in table 4.9 and 4.10 respectively.

Table 4.9 Strength values and failure mode of split-ring joints of series 5 (= 28.8 kN).

Specimen No.	F_{max} (kN)	Failure mode
DRa 101	30.13	shear plug of middle member
DRa 102	28.91	shear plug of middle member
DRa 103	-	Failed during the creep test
DRa 104	30.57	shear plug of middle member
DRa 105	27.84	shear plug of middle member
	F_{avg} = 29.36 kN, std = 1.23 kN, cov = 0.04	

Table 4.10 Strength values and failure mode of split-ring joints of series 4 (= 28.8 kN).

Specimen No.	F_{max} (kN)	Failure mode
DRa 111	23.13	shear plug of middle member
DRa 112	26.10	shear plug of middle member
DRa 113	30.82	shear plug of middle and side member
DRa 114	29.43	shear plug of middle member
DRa 115	43.86	cross section failure in side member
	F_{avg} = 30.67 kN, std = 7.96 kN, cov = 0.26	

Due to the high strength of specimen DRa 115 the coefficient of variation of specimens DRa 111 to 115 becomes 0.26. This specimen failed due to shear / cross section failure of a side member while all other specimens failed by means of shear plug of the middle member. The middle member of DRa 115 showed very thin growth rings as compared to the side members, which will have contributed to this higher strength.

Despite this single result, it can be concluded that shear plug is the most common failure mode in split-ring joints with this geometry. The average strength of 30.67 kN is however in good agreement with the average value of 29.36 kN of specimens DRa 101 to 105. Shear plug is also the dominant failure mode in time to failure tests so it can be concluded that no change in failure mode occurs due to the previous creep test.

4.3 *Influence of density on the joint strength*

To check whether the density of the boards in the joints has an influence of the joint strength an analysis has been performed. The average density of a joint was determined as the mean value of the boards of which the joints were manufactured. Each joint was manufactured from two boards, one for the middle member and one for the two side members. The load carrying capacity as a

function of the density is shown in figures 4.8 to 4.10 for the nailed, toothed-plate and split-ring joints respectively.

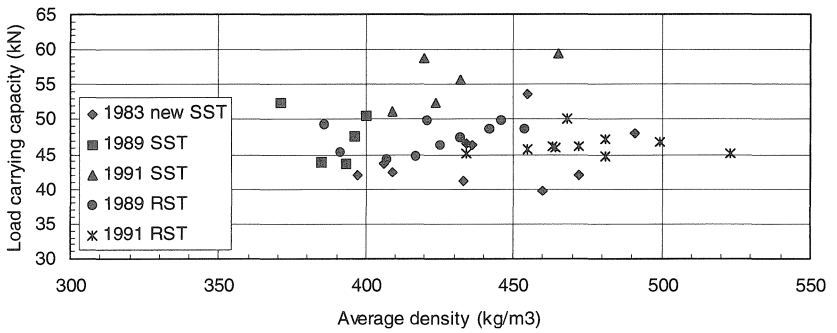

Fig. 4.8 Influence of density on the load carrying capacity of nailed joints.

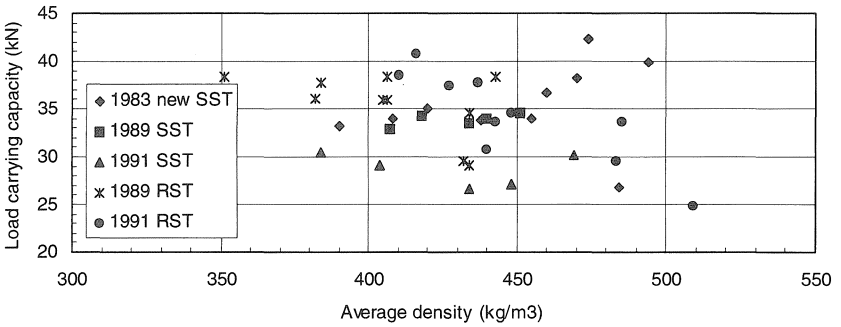

Fig. 4.9 Influence of density on the load carrying capacity of toothed-plate joints.

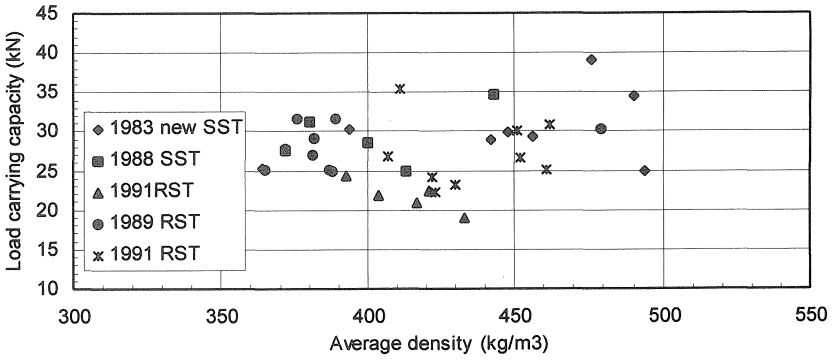

Fig. 4.10 Influence of density on the load carrying capacity of split-ring joints.

It can be concluded that the density of the timber has no influence on the load carrying capacity of the joint types studied here.

4.4 *Relative strength for all test series*

The relative strength of the joints has been determined by dividing the average strength of each of the series by the average short term strength of non-preloaded joints.

Table 4.5 Results of the RST tests on preloaded joints (kN) and relative strength value.

	nails	relative strength	toothed-plate	relative strength	split-ring	relative strength
SSD	45.0	-	32.2		28.8	
series 1	45.9	1.02	35.0	1.09	27.3	0.95
series 2	47.5	1.05	35.4	1.10	28.1	0.98
series 3	46.3	1.03	34.1	1.06	27.2	0.94
series 4	61.6*	1.37	35.7	1.11	30.7	1.07
series 5	49.7	1.10	38.0	1.18	29.4	1.02

* Series with rusted nails.

In almost every case the residual capacity ratio is equal to or higher than 1, indicating an increase in load carrying capacity as compared to the standard short term tests. Only three series of the split-ring joints give a ratio lower than unity but the deviation from unity is less than 6%.
In figure 4.11 the strength ratios are shown as a function of the preloading time.

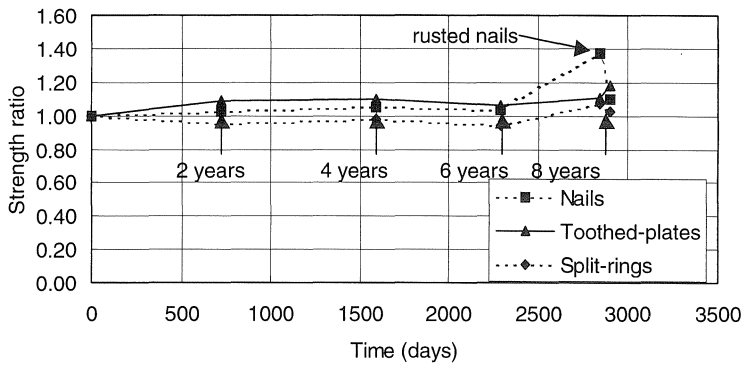

Fig. 4.11 Strength ratios after loading periods between 700 and 3000 days.

It must be kept in mind that figure 4.11 does not give the accumulated load, since the various series have been subjected to different loading sequences. It can be concluded from these test series the the full strength of the joints remains available during these tests.

5 Prediction of the residual capacity by damage accumulation models

5.1 *Introduction*

Since the creep load will lead to failure at some point in time, it is interesting to know how the load carrying capacity of the specimen develops during the test. From the test results it is known that the specimen's load carrying capacity remains at 100% for many years. At the same time is recognized that joints at load levels of 50% may fail during loading periods of up to 8 years. Apparently at some point in time the load carrying capacity starts to decrease until the remaining capacity is reduced to a level equal to the applied load. At that point in time the specimen fails. A generally accepted method to describe the strength development in time is to make use of damage accumulation models. Many different models are described in the literature and a good overview of available models can be found in Hwang and Han [1986]. Most discussed models were developed for fatigue phenomena in steel and fibre reinforced materials. None of the models traditionally used for timber were incorporated in Hwang and Han and they will be discussed here. In the discipline of timber engineering a distinction is made between "American" and "Canadian" damage models, due to the nationality of the respective authors. In the following the "American" damage model will be used which is an exponential damage accumulation function for the nailed, toothed-plate and split-ring joints. For comparative reasons the Canadian damage model of Foschi and Yao [1986, 1989] has also been applied to toothed-plate joints.

The basic principle of damage models is that a damage parameter is introduced. This parameter describes the amount of damage in the material at a time t. In the beginning the damage parameter is 0. A value of 1 is associated with failure and thus: $0 \leq \alpha \leq 1$. Intermediate stages are associated with a decrease in material strength. An increase in the value of gives a decrease in load carrying capacity. The decrease in capacity could be caused for example by a crack that has increased in size, but has not yet led to failure of the whole specimen. The net area for transfer of stresses thus decreases and the specimen strength decreases.

All major studies have focused on the verification of damage models at time to failure. The development of the strength before failure has only gained limited attention and remains difficult. In Morlier et al [1994] it is stated that it is not possible to measure the amount of damage. However, with an appropriate series of tests it is possible to monitor the development of the strength in time. This is possible by testing specimens in a short term test, which have previously been tested in a creep test at a load level σ_c. Using creep tests with different time durations the development of the strength in time can be investigated even at different or changing load levels. The wording "strength development" is chosen instead of strength decrease. It does not necessarily have to be a decrease in strength. If low loads are applied, it is possible that the accumulated damage is counteracted by an aging effect which may lead to a strength increase rather than a decrease.

5.2 *The exponential damage model*

Gerhards [1979, 1987, 1988] published a cumulative damage model of the following form:

$$\frac{d\alpha}{dt} = \exp\left(-a + b\frac{\sigma(t)}{\sigma_s}\right) \tag{1}$$

where σ_s is the average standard short term strength. Model constants a and b are parameters to be fitted from experiments. The equation can be solved for constant loading rate as well as constant load (creep to failure). For the load durations used in the test series the uploading stage can be neglected compared to the creep stage. Thus equation (1) can be solved with $\sigma(t) = \sigma_c$ for a creep test:

$$d\alpha = \exp\left(-a + b\frac{\sigma_c}{\sigma_s}\right)dt \tag{2}$$

and integration gives:

$$\alpha = t \cdot \exp\left(-a + b\frac{\sigma_c}{\sigma_s}\right) \tag{3}$$

Failure occurs when $t = T_c$, then $\alpha = 1$:

$$1 = T_c \cdot \exp\left(-a + b\frac{\sigma_c}{\sigma_s}\right) \tag{4}$$

giving for the time to failure:

$$T_c = \exp\left(a - b\frac{\sigma_c}{\sigma_s}\right) \tag{5}$$

This equation can be written as a time to failure line in the following form:

$$\frac{\sigma_c}{\sigma_s} = c - d\ln T_c \tag{6}$$

Equation (6) is often used for time to failure analysis with T_c generally larger than 300 s. For the nailed, toothed-plate and split-ring joints these time to failure lines have been determined in Van de Kuilen [1999]. Consequently parameters a and b in equation (3) can be determined from c and d in equation (6).

The accumulated damage can be calculated for every load history. The accuracy of the calculation of the damage depends on the accuracy at which the parameters c and d of time to failure equation (6) has been determined. In the following figures 5.1 to 5.3 the development of the average load carrying capacity in time is shown for a constant load of 50% of the average short term strength of the three joint types.

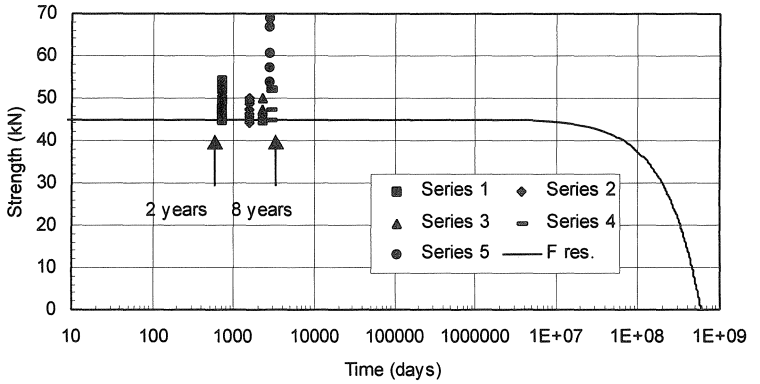

Fig. 5.1 Development of the average load carrying capacity of nailed joints.

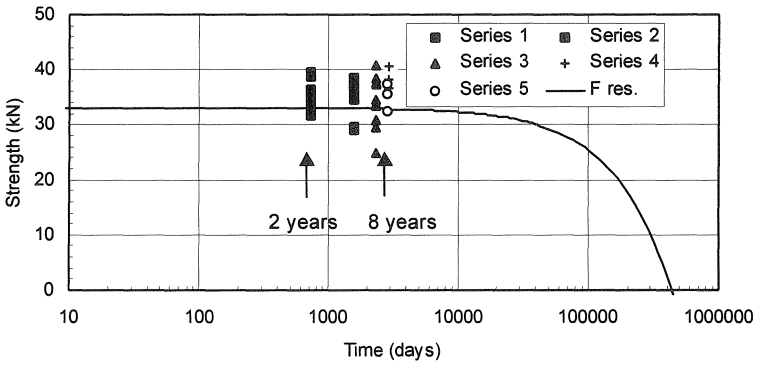

Fig. 5.2 Development of the average load carrying capacity of toothed-plate joints.

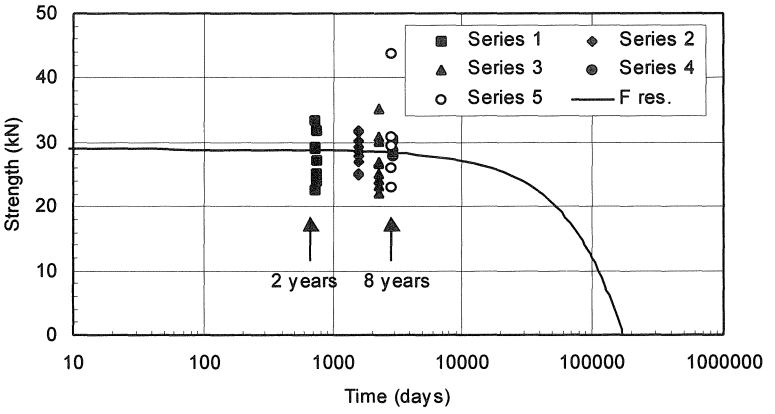

Fig. 5.3 Development of the average load carrying capacity of split-ring joints.

In Annex C the Foschi and Yao [1986] damage model has been applied to toothed-plate joints. The time to failure line of this model was fitted to the time to failure test results of the toothed-plate joints and the damage accumulation was calculated for the 50% load level.

It can be concluded from these graphs that the exponential damage equation predicts the load carrying capacity quite accurately, at least until the 8 years covered in the tests. Except for one split-ring joint which had failed during the creep test, all the other joints showed no reduction in the load carrying capacity. The large scatter in time to failure values at a single load level is important, since the residual load carrying capacity curve is based on the parameters of the time to failure line and consequently may be expected to have the same scatter.

6 Proposal for damage accumulation design

In the previous paragraphs it has been shown that the strength development in time can be written in the form of an exponential equation. In this paragraph the exponential damage equation will be used in a practical application.

$$d\alpha = \exp\left(-a + b\frac{\sigma_c}{\sigma_s}\right)dt \tag{7}$$

Integration in a time span t to $t + \Delta t$ gives the accumulated damage in Δt:

$$\Delta\alpha = \Delta t \cdot \exp\left(-a + b\frac{\sigma_{c;t}}{\sigma_s}\right) \tag{8}$$

Summation of $\Delta\alpha$ from 0 to T (the lifetime of the structure) requires that $\alpha < 1$. Equation (8) can be solved for periods Δt with a specified load σ_c. Numerical integration can be performed also.
The creep load σ_c has several components. Each type of load contributes during the lifetime for which the design has to be made. Contributions to σ_c can be expected from permanent load, life load, wind and snow. For simplicity these loads can be modelled as a step load. In a numerical integration procedure they can be time dependent. The duration of each of the load parts must be estimated.

Permanent load
The duration of the permanent load is equivalent to the design lifetime. In ordinary applications this design lifetime will be 50 years.

Wind load
The wind load will vary over the 50 years considerably. The average hourly wind speed v_h in the coastal area in the Netherlands is 5.2 m/s with a standard deviation σ_h of 2.7 m/s. The value is based on measurements at an elevation of 10 meters. The wind velocity can approximately be modelled using a Gumbel distribution in accordance with Vrouwenvelder and Vrijling [1987]. A Gumbel distribution can be shifted to determine other average values as for instance maximum hourly wind speed per year or per 50 years.

$$v_b = v_h + \left(\frac{\sqrt{6}}{\pi}\right)\left(\sigma_h \ln\left(\frac{t_b}{t_h}\right)\right) \tag{9}$$

The standard deviation does not change: $\sigma_b = \sigma_h$.

The average wind pressure can be calculated as:

$$q = \frac{1}{2}\rho v^2[1 + 2gI] \tag{10}$$

with:

q the wind pressure (N/m^2);
ρ air density (=1.25 kg/m^3);
v the wind speed (m/s);
$1+2gI$ factor taking into account the short term fluctuation depending on the roughness of the terrain (≈2.4).

The current design practice is based on the 50 year maximum hourly average. To determine this value a representative number of hours has to determined. This is not the number of hours in 50 years, since wind shows some degree of persistance. A representative number of hours per year is 1600 [Vrouwenvelder and Vrijling, 1987], which is 80000 hours for 50 years. With equation (9) the wind speed v_b can be determined at 29 m/s. The corresponding wind pressure is determined with equation 10 at 1260 N/m^2. This is the basic value for which structures are designed [NEN 6702, Eurocode 1 Part 2.4 Wind loads].

For the determination of damage accumulation the wind load is by way of example separated into four parts:

1. Average hourly wind speed for 50 years;
2. Maximum wind speed per year (6 hours per year over 50 years);
3. Maximum wind speed once in 50 years (6 hours).

Using equations 9 and 10 the following values for wind pressure and time duration can be derived.

Table 6.1 Wind load duration model.

Load category:	Wind speed: (m/s)	Pressure: (N/m^2)	Load duration: (hrs)
Wind load Q1	5.2	41	438000
Wind load Q2	20.7	640	300
Wind load Q3	29.0	1260	6

This leads to a graphical representation of the total load as shown in figure 6.1.

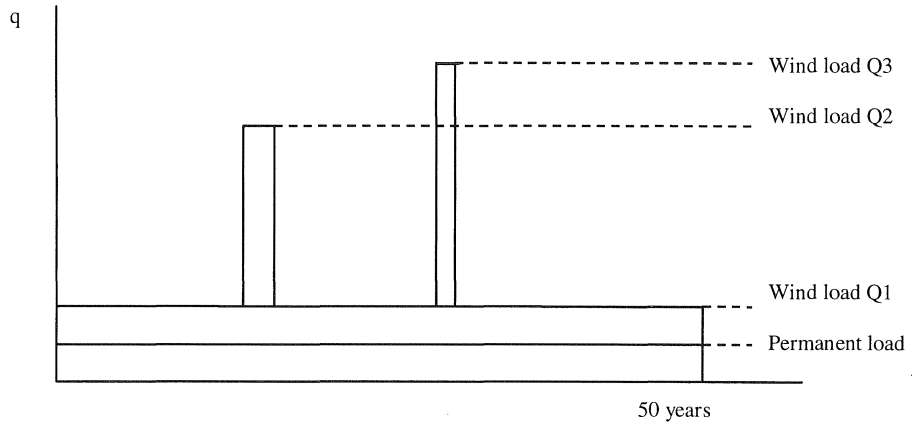

Fig. 6.1 Permanent and wind load block function for a period of 50 years.

Example

In the following example a toothed-plate tension joint is designed using a step-load function. The average load carrying capacity of the joint is 32.2 kN with a coefficient of variation 0.10. The characteristic load carrying capacity is calculated at 26.9 kN. The material factor is given in Eurocode 5: $\gamma_M = 1.3$. The modification factor for short duration of load is 0.9.

Design load carrying capacity:
The design load carrying capacity per toothed-plate connector, including the bolt:
$F_k * k_{mod} / \gamma_M = 26.9 * 0.9 / 1.3 = 18.6$ kN.

Permanent load:
The permanent load tensile force on the joint is determined at 10 kN. The load factor γ_p is assumed to be 1.35 in accordance with Eurocode 1.

Wind load:
The design wind load is based on a pressure of 1260 N/m^2. It is assumed that this pressure leads to a design tensile force of 28 kN. The load factor γ_q is assumed to be 1.5.

Design load combination:
$\gamma_G G + \gamma_q Q = 1.35*10 + 1.5*28 = 55.5$ kN.

A total of 55.5 / 18.6 = 2.98 = 3 toothed-plates are necessary.

Damage accumulation design

For the accumulation of damage the wind load was separated in three parts, the highest wind pressure giving a tensile force of 28 kN. Wind pressure $Q1$ and $Q2$ give loads of 0.94 and 14.7 kN respectively.

Equation (8) has been applied and figure 6.2 has been derived. The strength of the toothed-plate joint has been taken at 26.9 / 1.3 = 20.7 kN. In this case no k_{mod} factor has been applied since the duration of accumulated load is calculated through time integration of equation (8). On the right y-axis the accumulated damage α is shown. By definition, the joint is able to carry the load while α is smaller than 1.0.

The amount of toothed-plates which are necessary is derived at 2.92 compared to 2.98 in the current design method. Consequently, in both cases three toothed-plates are necessary.

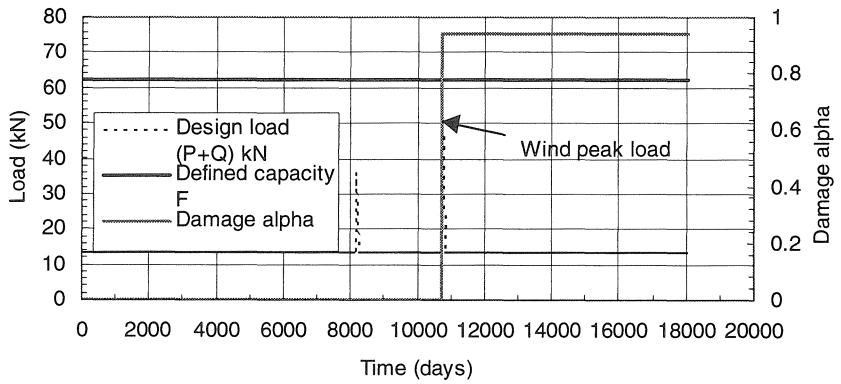

Fig. 6.2 Design of a joint using a damage accumulation design model.

The advantage of the damage accumulation design method becomes noticeable more clearly if a probabilistic approach is taken. The gain is mainly caused by a better description of the time span in which a maximum load is supposed to be acting.

In that case a graphical representation according to figure 6.3 is found. Wind load Q1 is taken as a random value with an average of 5.2 m/s +/- 2.7 m/s. This leads to a basic load of 0.98 kN +/– 0.5 kN over a period of 50 years. Furthermore the wind load peak is taken randomly in the 50 year time interval. This does not change the idea of the graphical presentation, except that the stepwise change in accumulated damage shifts in its position. The result is shown in figure 6.3. For the number of toothed-plates a value of 2.77 is found.

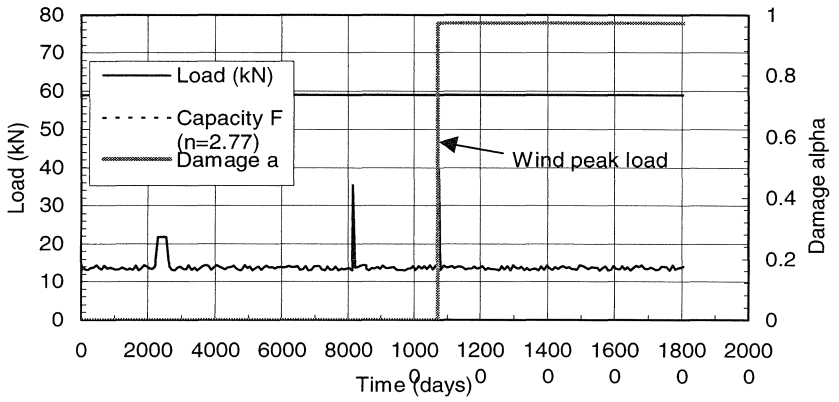

Fig. 6.3 Design of a joint using a damage accumulation design model and a random wind load.

It can be concluded that in this situation the γ_q factor of 1.5 is penalizing for the design method. High loads contribute more to the damage than low loads and using a γ_q factor of 1.5 during the full lifetime period overestimates the actual damage accumulation. As a result, the γ_q can be lowered during most of the lifetime and kept at 1.5 for the maximum load which is expected to occur. A probabilistic calculation can determine the actual value, which is expected to be in the order of 1.2.

7 Discussion and conclusions

Short term testing of timber joints that have been preloaded did not show a reduction in load carrying capacity. On the contrary, most test series showed an increase in average short term strength although the increase is small. One split-ring joint failed during the preloading period. This joint was loaded to 50% of the average short term strength. It is remarkable that failures may occur within a period of less than 8 years and that all other joints showed no reduction in load carrying capacity. Apparently the reduced load carrying capacity, prior to failure is short compared to total time under load. This very short failing period supports the use of damage models which predict 100% strength during most of the lifetime and rapid failure in the end. An exponential damage model as used here can describe such a strength curve as shown in paragraph 6. In case of toothed-plate joints partial failures may occur by shear plug formation under the bolt but the remaining time to total failure may still be considerable [Van de Kuilen, 1996]. In that case the damage equation can be adapted by using a time dependent strength in the damage equation.

The derived residual load carrying capacity curves seem to give a good indication of the actual capacity of specimens that have been under load for some time. The nailed joints indicate hardly any accumulated damage. The reason for this is that at load levels up to 65% of the average short

term strength no failures were found after testing times of more than 30 years. Consequently a time to failure line for nailed joints has a very gentle slope, which gives a very small value for parameter b in the damage equation. The time to failure lines for toothed-plate joints and split-ring joints are steeper compared to the nailed joints.

From the current test results it can be concluded that there is no reduction in load carrying capacity, and thus no noticeable damage accumulated yet, due to the preloading periods. It seems that there is even a slight possibility that the load carrying capacity is increased. A confirmation of this possible load carrying capacity increase is difficult to obtain but an increase in capacity after storage of unloaded joints was found by Palka [1985, 1986], who tested nail-plate joints. The scatter in test results from the short term tests is such that changes in residual load carrying capacity can be attributed to other factors than just capacity increase. This scatter can be due to different timber used in 1962 and the second series of 1983, a change in material properties due to the storage period, but also a change in the testing equipment and loading procedure or in the moisture content. Despite these possible differences, the conclusion can be drawn that no decrease in load carrying capacity has taken place during the loading periods reported here and that failures occur in time spans which are relatively short to the total time under load, with the exception of the toothed-plate joints.

A large increase in load carrying capacity is found from the nailed specimens with rusted nails. The specimens were soaked in hot water due to leakage of the heating system. The capacity increase can be attributed to increased withdrawal resistance of the nails in the final stage of the test. If the capacity ratio of this series is taken, an increase in load carrying capacity of more than 30% is obtained. Consequently, manufacturing timber structures with profiled nails increases competitiveness by either increasing the load carrying capacity of joints or decreasing the number of fasteners in the joint obtaining the same capacity.

If the failure mode of the 1994 RST tests on nailed joints are compared to the failure modes of short term tests it can be concluded that differences may occur. The creep load causes a displacement of the members relative to each other, but as long as this displacement is small, a short term test will result in a failure mode with two plastic hinges per nail. This is also the theoretically predicted failure mode. A cut through the RST tested specimens however, does not always show this nail bending pattern and both straight rotated nails as well as nails with one plastic hinge are observed. Furthermore, the creep load may result in splitting failure of the side members. This splitting is observed in specimens loaded to 50% or more. If a residual load carrying capacity test is performed on a specimen where splitting of the members is already present, it may be expected that the load carrying capacity is reduced. In the geometry tested here, it is expected that the long term resistance against splitting is governing instead of the long term embedding strength.

The conclusions reached here regarding the strength development in time are not in line with the conclusions reported by Leicester and Lhuede [1992]. Nail-plate joints showed severe strength reductions. The residual strength was 50 to 90% of the short term strength after periods to 10 years at load levels of only 20 to 30%. This means a strength loss of 10 to 50% after 10 years of testing. It is

unknown whether these 20 to 30% relates to the average short term strength or to the characteristic strength, but that does not influence the conclusion that severe strength losses may occur. Although times to failure of 10 years and less are not rare in the case of both toothed-plate and split-ring joints as shown in Van de Kuilen [1999], the reported strength losses are much larger. Apparently many of Leicester's joints that showed a strength loss must have partially failed already during the creep tests, similarly to the toothed-plate and split-ring joints that were tested in this study.

A proposal is done to use a simple damage accumulation equation for design purposes. To make better use of the possibilities of these damage accumulation equations it is necessary to obtain more accurate information on the time durations of maximum loads. The development of the damage α indicates the almost all the damage is developed during the occurence of the maximum (wind) loads. This is caused by the exponential behaviour of the damage equation. As such, optimisation of timber structures can be carried out by focussing on the duration of the highest expected loads during the lifetime of the structure.

Literature

Foschi, R.O., Yao, Z.C. Another look at three duration of load models. IUFRO S 5.02/CIB-W18/19-9-1 Meeting 19 Florence, Italy 1986

Foschi, R.O., Folz, B.R. Yao, Z.C. Reliability based design of wood structures. Structural Research Series, Report No. 34, Department of Civil Engineering, UBC, Vancouver, Canada, 1989.

Gerhards, C.C., Time related effects on wood strength. A linear cumulative damage theory. Wood Science, Vol. 11, No.3, pp. 139-144, 1979

Gerhards, C.C. Effect of grade on load duration of Douglas-fir lumber in bending. Wood and Fibre Science Vol 20(1), pp. 146-161, 1988.

Gerhards, C.C., Link, C.L. A cumulative damage model to predict load duration characteristics of lumber. Wood and Fibre Science, 19(2), 1987, pp. 147-164

Hwang, W, Han, K.S. Cumulative Damage Models and Multi-stress Fatigue Life Prediction. Journal of Composite materials, Vol. 20 - March 1986.

Johansen, K.W. Theory of Timber Connections. IABSE Publication No. 9. 249-262. Bern.

Kuipers, J, Kurstjens, P.B.J. Creep and Damage Research on Timber Joints - Part One. Stevin report 4-86-15/HD-23 Delft University of Technology, 1986.

Kurstjens, P.B.J. Creep and Damage Research on Timber Joints - Part Two. Stevin report 25.4-89-15/C/HD-24 Delft University of Technology, 1989.

Kurstjens, P.B.J. Creep and Damage Research on Timber Joints - Part Three. Stevin report 25.4-90-12/C/HD-26 Delft University of Technology, 1990.

Kurstjens, P.B.J., Stolle, P. Creep and Damage Research on Timber Joints - Part Four. Stevin report 25.4-91-06/C/HD-28 Delft University of Technology, 1991.

Leicester, R.H, Lhuede, E.P., Mechano-sorptive effects on toothed-plate connectors. IUFRO S5.02, Bordeaux, France, 1992.

Morlier, P., Creep in Timber Construction: Research needs, RILEM TC 112 Bordeaux, France, 1994.

PALKA, L.C. Effect of load duration upon timber fasteners: first data report, Forintek Canada Corp., 1985.

PALKA, L.C. Effect of load duration upon timber fasteners: second data report, Forintek Canada Corp., 1986.

VAN DE KUILEN, J-W.G. A time to failure analysis of toothed-plate joints. Stevinreport 4-96-4/HD-29, Delft University of Technology, 1996.

VAN DE KUILEN, J-W.G., H.J. Blass. Does damage accumulate in timber joints loaded at load levels below 50% of the average short term strength? IWEC, pp. 4.46-4.53, New Orleans, USA, 1996.

VAN DE KUILEN, J-W.G. Duration of load effects in timber joints, Ph.D. thesis (in print), Delft University of Technology 1999

VROUWENVELDER, A.C.W.M., Vrijling, J.K. Probabilistic design. Lecture Notes. Faculty of Civil Engineering, Delft University of Technology, 1987. (in Dutch)

Annex A Joint geometries

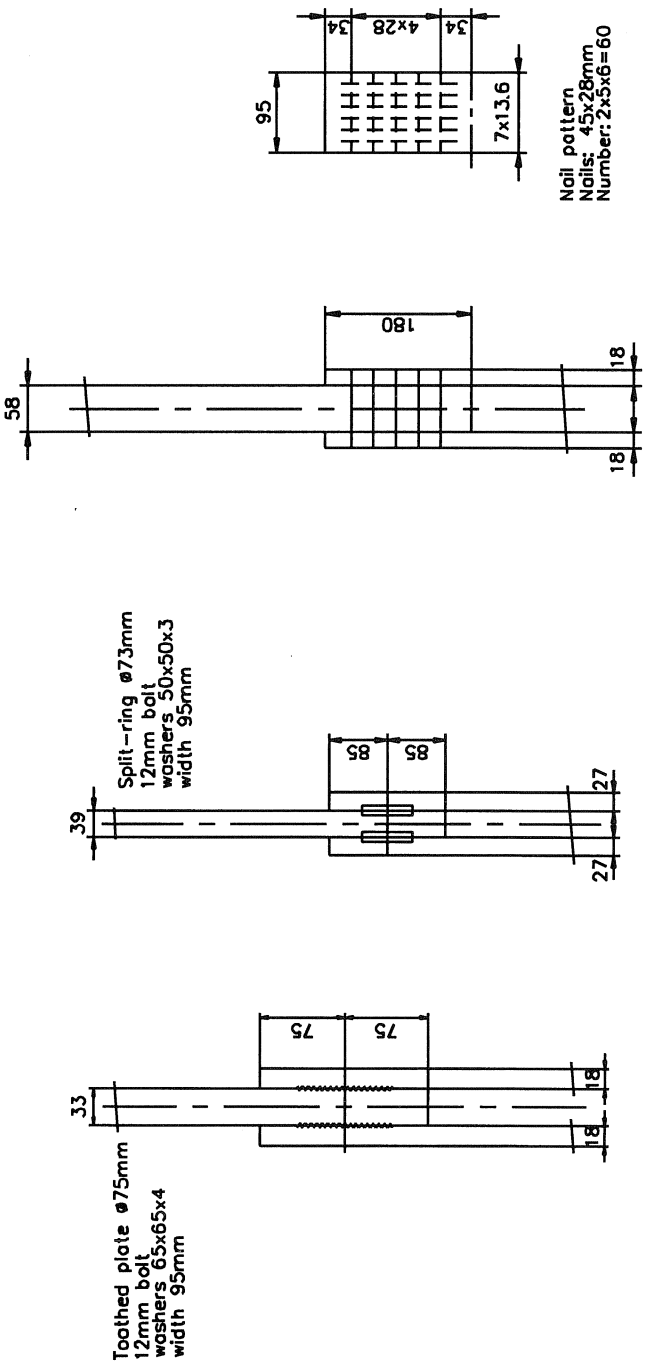

Annex B. Loading schedules of joints

Annex B.1 Loading schedules

Table B.1.1 Nailed joints 50% from 1984.

String number:	Series 1	Series 1
date of loading:	14-02-84	14-02-84
date of unloading:	04-02-86	04-02-86
duration of load:	17302 hours	17302 hours
	721 days	721 days
duration of recovery:	331 hours	331 hours
SSD test	03-03-86	05-03-86

Table B.1.2 Toothed-plate joints 50% from 1984.

String number:	Series 1	Series 1
date of loading:	30-01-84	30-01-84
date of unloading:	04-02-86	04-02-86
duration of load:	17659 hours	17659 hours
	735 days	735 days
duration of recovery:	331 hours	331 hours
SSD test	10-03-86	11-03-86

Table B.1.3 Split-ring joints 50% from 1984.

String number:	Series 1	Series 1
date of loading:	13-01-84	02-02-84
date of unloading:	04-02-86	04-02-86
duration of load:	18071 hours	17590 hours
	752 days	733 days
duration of recovery:	331 hours	331 hours
SSD test	12-03-86	13-03-86

Annex B.2 Loading schedules

Table B.2.1 Nailed joints and toothed plate joints: 40-50% from 1984.

String number:	Series 2	Series 2
date of loading to 40%:	09-02-84	23-02-84
date of unloading:	10-06-86	10-06-86
duration of load:	20423 hours	20109 hours
	851 days	837 days
recovery till:	21-08-86	25-08-86
duration of recovery:	1730 hours	1826 hours
	72 days	76 days
date of uploading to 50%:	21-08-86	25-08-86
date of unloading:	29-08-88	29-08-88
duration of load:	17735 hours	17638 hours
	739 days	735 days
recovery till:	02-01-89	02-01-89
duration of recovery:	3002 hours / 125 days	3002 hours / 125 days
SSD test	25/26-01-89	31-01/01-02-89

Table B.2.2 Split-ring joints: 40-50% from 1984.

String number:	Series 2	Series 2
date of loading to 40%:	16-02-84	23-02-84
date of unloading:	10-06-86	10-06-86
duration of load:	20253 hours	20109 hours
	844 days	837 days
recovery till:	21-08-86	25-08-86
duration of recovery:	1730 hours	1826 hours
	72 days	76 days
date of uploading to 50%:	21-08-86	25-08-86
date of unloading:	29-08-88	29-08-88
duration of load:	17735 hours	17638 hours
	739 days	735 days
recovery till:	02-01-89	02-01-89
duration of recovery:	3002 hours	3002 hours
	125 days	125 days
SSD test	27-01-89	31-01-89

Annex B.3. Loading schedules

Table B.3.1 Nailed, toothed plate and split-ring joints: 30-40-50% from 1984.

String number:	Series 3 Nailed	Series 3 Toothed-plate	Series 3 Split-ring
date of loading to 30%:	27-03-84	27-03/03-04-84	14/15-03-84
date of unloading:	11-06-86	11-06-86	11-06-86
duration of load:	19680/19656 hrs. 820/819 days	19368/19176 hrs. 807/799 days	19369 hrs. 807 days
recovery till:	26-08-86	26-08-86	26-08-86
duration of recovery:	1825 hours 76 days	1824 hours 76 days	1824 hours 76 days
date of uploading to 40%:	26-08-86	26-08-86	26-08-86
date of unloading:	07-09-88	07-09-88	07-09-88
duration of load:	17832 hours 743 days	17832 hours 743 days	17832 hours 743 days
recovery till:	20-02-89	20-02-89	20-02-89
duration of recovery:	3983 hours 166 days	3983 hours 166 days	3983 hours 166 days
date of uploading to 50%:	20-02-89	20-02-89	20-02-89
date of unloading:	20-02-91	18-02-91	19-02-91
duration of load:	17495 hours 729 days	17472 hours 728 days	17520 hours 730 days
recovery:	none	none	none
SSD test	25/26-01-89	31-01/01-02-89	

Annex B.4. Loading schedules

Table B.4.1 Nailed, toothed plate and split-ring joints: 30-40-50% from 1986.

String number:	Series 4 Nailed	Series 4 Toothed-plate	Series 4 Split-ring
date of loading to 30%: split-rings 45%	21-08-86	20/21-08-86	20-08-86
date of unloading:	06-09-88	06-09-88	06-09-88
duration of load:	776 days	776 days	776 days
recovery till:	15-02-89	15-02-89	15-02-89
duration of recovery:	70 days	70 days	70 days
date of uploading to 40%:	15-02-89	15-02-89	15-02-89
date of unloading:	12-04-91	12-04-91	12-04-91
duration of load:	786 days	786 days	786 days
recovery till:	19-04-91	19-04-91	19-04-91
duration of recovery:	7 days	7 days	7 days
date of uploading to 50%:	19-04-91	19-04-91	19-04-91
date of unloading:	15-09-94	15-09-94	15-09-94
duration of load:	1281 days	1281 days	1281 days
recovery:	none	none	none
SSD test	22-09-94	22/25-09-94	25-09-94

Annex B.5. Loading schedules

Table B.5.1 Nailed, toothed plate and split-ring joints: 50% from 1986.

String number:	Series 5 Nailed	Series 5 Toothed-plate	Series 5 Split-ring*
date of loading to 50%:	10-11-86	10-11-86	10-11-86
date of unloading:	15-09-94	15-09-94	15-09-94
duration of load:	2896 days	2896 days	2896 days
recovery:	none	none	none
SSD test	22-09-94	22/25-09-94	25-09-94

* One split-ring specimen failed on 01-09-88 giving a time to failure of 738 days.

Annex C

Damage accumulation in toothed-plate joints loaded to 50%.